

Ultrafast Quantum Optics and Communication

Mohamed Sennary¹, Javier Rivera-Dean², Mohamed ElKabbash³, Vladimir Pervak⁴, Maciej Lewenstein^{2,5}, Mohammed Th. Hassan^{*1,3}.

¹ Department of Physics, University of Arizona, Tucson, AZ 85721, USA.

² ICFO–Institut de Ciències Fòniques, The Barcelona Institute of Science and Technology, Castelldefels (Barcelona) 08860, Spain.

³ James C. Wyant College of Optical Sciences, University of Arizona, Tucson, Arizona 85721, USA

⁴ Ludwig-Maximilians-Universität München, Am Coulombwall 1, 85748, Garching, Germany.

⁵ ICREA, Pg. Lluís Companys, 23, 08010 Barcelona, Spain.

*Corresponding author Email: mohammedhassan@arizona.edu.

Advancements in quantum optics and squeezed light generation have revolutionized various fields of quantum science over the past three decades, with notable applications such as gravitational wave detection. Here, we extend the use of squeezed light to the realm of ultrafast quantum science. We demonstrate the generation of ultrafast, broadband quantum light pulses spanning 0.33 to 0.73 PHz using light field synthesizer and a four-wave mixing nonlinear process. Experimental results confirm that these pulses exhibit amplitude squeezing, which is consistent with theoretical predictions. This work lays the groundwork for a new field of ultrafast quantum science, enabling real-time studies of quantum light-matter interaction dynamics, which expect to reveal new physics. We also demonstrate the encoding of binary digital data onto these quantum light waveforms, synthesized with attosecond resolution, showcasing potential applications in secure quantum communication. This work paves the way for ultrafast quantum optoelectronics, quantum computing, and next-generation encrypted quantum communication networks, capable of achieving petahertz-scale data transmission speeds.

Over the past few decades, significant advances in quantum optics, particularly the generation of quantum light¹⁻³, have played a pivotal role in enhancing the sensitivity of gravitational wave measurements by the Laser Interferometer Gravitational-Wave Observatory (LIGO)^{4,5}. Concurrently, the evolution of ultrafast science, attosecond physics, and the development of cutting-edge tools—such as femtosecond high-power lasers and XUV pulses—have spurred new frontiers in both fundamental research and technological applications. These breakthroughs, acknowledged by the Nobel Prizes in Physics in 2018 and 2023, have enabled detailed investigations into light-matter interactions at the classical level, thereby providing

profound insights into molecular, atomic, and electron dynamics⁶. For instance, attosecond science has leveraged the high-harmonic generation (HHG) to probe electron motion on timescales as short as attoseconds⁷⁻¹². Recent experimental and theoretical studies have explored the impact of squeezed quantum light on HHG process, revealing that the underlying physics of HHG with squeezed light deviates significantly from classical descriptions¹³⁻²². Theoretical models predict shifts in both the electronic trajectories driven by the field and the emitted photon energy compared to those observed under coherent laser fields²³. Experimental demonstrations of HHG^{22,24} in solid-state materials using squeezed light have also shown promising results, yielding higher photon fluxes^{13,25}.

Additionally, the control of electron and XUV photon statistics through different quantum light modes has been reported, suggesting the potential for tailored quantum control in ultrafast processes^{22,26}. These findings raise critical questions: How do light-matter interactions and ultrafast phenomena evolve when triggered by squeezed light? How do the physics of ultrafast nonlinear optics differ when using quantum light? Addressing these questions calls for new novel tools—specifically, ultrafast quantum light pulses—that can offer a new window into ultrafast science through the lens of quantum physics.

In this work, we present a novel approach for generating ultrafast quantum-synthesized few-cycle pulses produced via a nonlinear four-wave mixing process using a pulse synthesized by our light field synthesizer. The resulting quantum light pulse exhibits intensity squeezing at the cost of phase uncertainty, as confirmed by both experimental and theoretical analyses. With a pulse duration of 5.3 fs, these pulses represent a promising tool for a range of advanced applications, including ultrafast quantum optics and spectroscopy aimed at exploring light-matter interactions at the quantum level. Moreover, the amplitude squeezing inherent in these pulses enhances the signal-to-noise ratio, surpassing the performance of classical light sources²⁷, with promising applications in ultrafast spectroscopic studies of biological samples^{28,29}.

The amplitude squeezing inherent in these pulses also enhances the signal-to-noise ratio in ultrafast spectroscopic studies of biological samples, surpassing the performance of classical light sources. Furthermore, the ability to precisely control the waveform of these quantum pulses opens new avenues for investigating and manipulating electron dynamics in materials, providing a platform for comparing electron motion driven by quantum versus classical light.

As an initial demonstration of the potential significance of these synthesized quantum pulses, we present a secure ultrafast quantum communication scheme, leveraging the digital encoding on ultrafast waveforms. Beyond the inherent security of squeezed light in quantum communication, our synthesized quantum pulses introduce an additional layer of digital encryption where the data are carried on the squeezed ultrafast light waveform in the binary format of (0 & 1). This approach establishes a foundational framework for advancing ultrafast quantum science with transformative potential across diverse scientific and technological domains. The demonstrated capabilities of ultrafast quantum applications also pave the way for developing next generation petahertz quantum electronics and communication protocols.

Ultrafast quantum light

In previous studies, we demonstrated the generation of ultrafast synthesized coherent light pulses using the light field synthesizer (LFS)³⁰⁻³⁴. The outline of LFS is shown in Fig. 1a, and further details of our experiment setup are discussed in Methods. The synthesis process involves splitting a broadband supercontinuum into three distinct components—near-infrared (NIR), visible (VIS), and ultraviolet (UV)—using dichroic beam splitters (DBSs). The temporal profiles of these pulses are measured and presented in Fig. S1. These pulses (see Fig. S1) are then coherently recombined using DBSs, forming a broadband few-cycle coherent light pulse, which serves as the LFS output. The pulse waveform is synthesized and dynamically tailored by adjusting the relative delays and intensities of the constituent pulses. In our experiment, the output beam is split by a beamsplitter (BS) into two beams: one beam is directed into spectrometer #1 for broadband spectral analysis. The spectrum of this coherent broadband pulse is shown in Fig. 1b, and the constituents' spectral channels are plotted in Fig. 1c. The other beam is used for quantum light generation by focusing this beam onto a 100 μm tilted SiO_2 target, where four-wave mixing (FWM) generates squeezed light in the amplitude (intensity) quadrature. The conversion efficiency is estimated to be in the order of 0.1%, which depends on the nonlinear material and thickness as well as the input beam intensity. The squeezed light is isolated through a one-hole mask and recorded by spectrometer #2. The resulting spectrum spans approximately 0.33 to 0.73 PHz (Fig. 1d), with the constituent pulse spectra shown in Fig. 1d.

To validate amplitude squeezing in this broadband nonlinear signal, we employ an approach distinct from the conventional method used for continuous wave (CW) lasers. By exploiting spectral interference between temporally delayed constituent pulses (NIR-VIS and VIS-UV), we measure phase ($\Delta\phi$) and intensity (ΔI) uncertainty. It is important to clarify that ($\Delta\phi$) here correspond to the field phase uncertainty while the amplitude quadrature uncertainty (ΔI) refers to the uncertainty in the photon count over the entire synthesized light. Crucially, the field phase uncertainty and the amplitude noise are obtained from different measurements. The phase jittering is obtained from interference fringes within the spectral overlap region (insets in Fig. 1c and e), while intensity stability is obtained through measuring the variance in the overall pulse intensity.

Amplitude squeezing is confirmed when the intensity fluctuations of the nonlinear signal, I_q , are smaller than those of the coherent light, I_c (i.e., $\Delta I_q < \Delta I_c$), while phase jittering of the squeezed light, $\Delta\phi_q$, exceeds that of the coherent light, $\Delta\phi_c$ (i.e., $\Delta\phi_q > \Delta\phi_c$). Thus, we performed phase and intensity measurements on the NIR-VIS (Fig. 2a-b) and VIS-UV (Fig. 2c-d) pulse pairs. The NIR-VIS measurements involved delaying the NIR and VIS pulses and measuring phase jittering through Fourier analysis of the spectral interference fringes, with results shown in Fig. 2aI and aII. For the amplitude quadrature uncertainty, we normalized to the average intensity of the measured spectra (contains all the frequencies of both VIS and NIR pulses to compensate for any difference in the power between the coherent and squeezed lights). Then, we calculated the relative intensity change ΔI and plotted it in Fig. 2bI and bII.

Similarly, the phase jittering and intensity changes for the VIS-UV pair were measured and plotted in Fig. 2cI and cII and Fig. 2dI and dII, respectively. Dark noise from the spectrometers (Fig. S2) was negligible, being two orders of magnitude lower than the observed amplitude fluctuations.

Our findings, summarized in Fig. 2, reveal that the phase uncertainty is higher in the squeezed light (Fig. 2aII and cII) compared to the coherent light (Fig. 2aI and cI), while the amplitude of the squeezed light (Fig. 2bII and dII) is more stable than that of the coherent light. These results confirm that the generated quantum light from the FWM process is amplitude-squeezed at the expense of increased phase uncertainty. Although, the squeezing is measured at the overlapping spectral region between the channels, the amount of squeezing for the separate channels should be effectively the same due to the collinear phase matching at FWM. To assess amplitude stability for individual pulse components, we spectrally filtered the constituent pulses and measured their intensity stability. Results from the NIR-VIS and VIS-UV measurements (retrieved from Fig. 2b and D and plotted in Fig. S3 and S4) indicate that the amplitude stability difference between the squeezed and classic light of the different channels is roughly comparable between the NIR-VIS pulses, and the UV-VIS pulses. Amplitude squeezing is achieved through the quantum correlations induced by the nonlinear four-wave mixing interaction between the three input beams. In our experiment, the incident angle of the three beams is very small ($<5^\circ$), which enables optimal phase matching and constructive interference (i.e., reduced uncertainty in the number of photons generated). However, these generated photons introduce increased randomness in the timing of their generation, which in turn leads to increased uncertainty in the carrier phase.

Theoretical Modeling and the Wigner function of the ultrafast squeezed light

We developed theoretical models to simulate the squeezing observed in our experiments, allowing us to compare the experimental findings with experiment outcomes. From a theoretical point of view, the four-wave mixing process under co-linear phase matching conditions and within the parametric approximation³⁵ produces squeezed coherent states of the form $\hat{S}(r_i)|\alpha_i\rangle$. In this expression, N denotes the number of modes, $S(r) = \exp[ra^2 - r^*a^\dagger{}^2]$ is the squeezing operator, and $|\alpha\rangle$ represents a coherent state of light. To determine the compatibility of the experimental results with these theoretical squeezed states, we compared the variances in phase and intensity obtained experimentally, $\Delta\Phi_{exp}^2$ and ΔI_{exp}^2 , with the theoretical predictions, $\Delta\Phi_{th}^2(\mathbf{x})$ and $\Delta I_{th}^2(\mathbf{x})$, (see Ref. [36] and the supplementary information (SI) for detailed calculations), the latter parametrized by $\mathbf{x} = \{(r_i, \alpha_i)\}_{i=1}^N$. Specifically, we defined the following function

$$C(\mathbf{x}) = A[\Delta I_{th}^2(\mathbf{x}) - \Delta I_{exp}^2]^2 + B[\Delta\Phi_{th}^2(\mathbf{x}) - \Delta\Phi_{exp}^2]^2, \quad (1)$$

which serves as a measure of the distance between the experimental observations and the theoretical expectations, where a value of $C(\mathbf{x}) = 0$ would represent a perfect match between the two. Consequently, the comparison involves finding an optimal set of parameters \mathbf{x}^* that

minimizes Eq. (1) as much as possible. To achieve this, the parameters A and B have to be chosen carefully to ensure simultaneous minimization of both terms within the function. In practice, the optimization was performed across a range of values for A and B , and the best result was retained (see SI for more details). Furthermore, given that the experimental data suggests the presence of amplitude-squeezing, we restricted our search-space to real values of r_i and α_i when solving this optimization problem, as to reduce the number of variables over which to optimize.

The results from this optimization are shown in Fig. 3a and b as a function of the number of modes N , where Fig. 3a represents the IR-Vis dataset and Fig. 3b the UV-VIS dataset. The dashed curves show the absolute difference between the experimental and theoretical variances after optimization, while the solid horizontal lines represent the experimental variance values. In all cases, we observe that the dashed curves lie below their respective solid horizontal lines—indicated in matching colors—demonstrating a good agreement between theory and experiment, as the absolute error remains around one and two orders of magnitude below the experimental values. Notably, this trend persists across all values of N considered in our study, suggesting that the experimental data is compatible with the presence of squeezed states along multiple modes. However, for both the IR-Vis and UV-VIS datasets, an increase in the number of modes generally corresponds to reduced accuracy in the absolute error, particularly pronounced in the intensity variance. In overall terms, we observe that the best results are achieved in the $N=1$ case, yielding a total amount of estimated squeezing of 13.03 dB for the IR-Vis dataset and 8.81 dB for the UV-VIS dataset. The difference in the squeezing level maybe attributed the alignment optimization in two measurements to achieve the optimized FWM output signal. The Wigner function³⁷ of the resulting squeezed states are shown in Fig. 3c & d, respectively, where χ and p represent the optical quadratures. The functions have been rotated by 45° relative to the p -axis for representational purposes. They correspond to a Gaussian distribution that has been squeezed along one optical quadrature and expanded along the conjugate quadrature.

Ultrafast quantum-encrypted digital communications

Next, in our experiment, we coherently superimpose the squeezed light generated by the three channels of our light field synthesizer (LFS) to produce ultrafast quantum laser pulses. These squeezed light pulses are focused into a thin SiO₂ plate, and we sampled the waveforms using the all-optical field sampling technique previously developed by our group^{30,31}. The measured squeezed light waveform and intensity profile are shown in Fig. 4a and b (see detailed explanations in SI). The full width at half-maximum (FWHM) duration of this ultrafast squeezed light pulse is 5.3 fs, with pulse dispersion not fully compensated, close to the pulse duration of the classic light pulse measured by FROG approach (see Fig. S1c).

In previous work, we employed complex waveforms—synthesized by controlling the relative delay between the constituent pulses in LFS—of coherent light for digital data encoding (binary 0 and 1), which could be applied to ultrafast communication systems³⁸. This technique involved synthesizing arbitrary waveforms using the LFS to represent binary sequences, which were subsequently decoded by focusing the synthesized light onto a dielectric medium (e.g., SiO₂) and

measuring the real-time modulation of the reflected optical intensity, with the intensity threshold set as agreed upon between the parties ³⁹. Building on this approach, we now extend the methodology to use squeezed ultrafast light waveforms for quantum communication.

Continuous-variable quantum key distribution (CV-QKD) typically relies on encoding information into the quadratures of quantum states, such as amplitude (ΔI) and phase ($\Delta\phi$), using a squeezed or coherent light source. The receiver (Bob) measures one of these quadratures using a local oscillator (LO) to project the quantum state onto the desired quadrature, chosen at random. The security of CV-QKD arises from the inability of an eavesdropper (Eve) to intercept the quantum state without introducing detectable noise, owing to the Heisenberg uncertainty principle.

In our petahertz communication scheme, the waveforms of the ultrafast synthesized squeezed light are used to encode quantum-encrypted digital data, as illustrated in Fig. 5. In this setup, Alice (Fig. 5a) synthesizes and encodes digital data onto amplitude-squeezed light waveforms using the LFS (Fig. 5a I-III). The measured exemplary waveforms shown in Fig. 5a I-III are average of three scans and despite the phase uncertainty of these waveforms they maintain their shapes. Alice sets a predefined intensity threshold (30%) for the modulation, encrypting the data within the squeezed waveforms. She then sends the encoded squeezed light beam to Bob (Fig. 5b), sharing the squeezing degree and the threshold information. As in conventional CV-QKD, any eavesdropping attempt by Eve (Fig. 5c) to intercept and decode the squeezed light waveform would alter its squeezing degree, thereby revealing the intrusion to both Alice and Bob. Bob can check the signal's squeezing degree by measuring its intensity stability between different pulses (as we did in our experiment, as shown in Fig. 2) to confirm the communications security.

Nonetheless, the measurement of the uncertainty in intensity and phase across the entire spectrum of the signal could make the communication vulnerable to a resend attack ⁴⁰. To address this, we suggest that Alice uses one of the three pulses in the LFS—specifically, the NIR pulse—as a quantum-correlated local oscillator ⁴¹. This eliminates the need for an external classical LO and simplifies synchronization. At the receiver station, after sampling the waveform and decoding the digital data, Bob introduces a controllable relative time delay between the NIR reference pulse and the other pulses. This delay adjusts the interference conditions at specific wavelengths, allowing Bob to effectively select quadrature projections by inducing constructive or destructive interference. By varying the delay, Bob dynamically selects which quadrature component (amplitude or phase) to measure at a given wavelength. He then measures the noise at specific wavelengths within the spectral overlap region, where spectral interference exists between the different channels. Depending on the interference condition at that wavelength, Bob measures a specific quadrature and obtains the squeezing level of the selected quadrature projection. This protocol enhances security by making it difficult for an eavesdropper to predict Bob's quadrature choices or replicate the quantum-correlated states without introducing detectable noise. This approach avoids challenges associated with classical LOs, enables dynamic quadrature selection, and leverages quantum correlations to strengthen the security and efficiency of CV-QKD.

Remarkably, our protocol introduces additional layers of security, in analogy to the typical CV-QKD protocol, protecting the communication from potential tampering. Specifically, our approach

provides multiple safeguards against Eve's interference: (i) Eve would need the decoding key to correctly interpret the transferred information, (ii) Eve cannot accurately decode the data without knowing the predefined intensity threshold (30%), and (iii) even if Eve knows the threshold, her measurement of the squeezed light waveform using a beamsplitter will inevitably disturb the squeezing, introducing errors in the decoded data due to the altered squeezing degree. This disturbance increases the tolerance error of the pre-defined threshold and amplifies the likelihood of faulty decoding, as shown in Fig. 5 cI-III. Consequently, our approach not only secures the communication channel but also protects the transferred data from unauthorized retrieval. This ultrafast quantum communication protocol operates at data transfer rates in the petahertz/second,

Although, our petahertz quantum communication protocol offers a higher level of security due to the intrinsic sensitivity of squeezed light to any eavesdropping attempt, there are practical challenges, such as maintaining low-loss transmission of squeezed pulses over long distances operating. Scaling up the LFS and the input coherent laser pulse power to generate a high-power squeezing synthesized pulse would overcome the transmission loss problem and supports a robust ultrafast quantum communication. Furthermore, achieving the quantum communication with the petahertz frequency speed is currently limited only by the laser repetition rate and the delay stage speed in the synthesizer. However, with ongoing advancements in ultrafast optoelectronics and laser technologies, this digital data speed is potentially on the horizon ³⁹.

This work introduces a groundbreaking approach to ultrafast quantum optics by demonstrating the generation of broadband squeezed light pulses with attosecond precision. By leveraging these ultrafast quantum light waveforms, we have shown how they can be used for secure quantum communication, marking a significant step toward the realization of high-speed, encrypted communication networks. Our results not only open new avenues for exploring quantum light-matter interactions in real time but also lay the foundation for future advancements in ultrafast quantum optoelectronics and quantum computing. As quantum communication systems evolve, the ability to operate at petahertz-scale data transmission speeds will be critical, and our findings contribute to the development of technologies that can meet these challenges while ensuring security and robustness. The potential of ultrafast squeezed light in secure communication represents a promising frontier for both fundamental research and practical applications in the quantum technology landscape.

Methods

In our experimental setup, few-cycle laser pulses centered at 750 nm (passively stabilized carrier-envelope phase) are generated by an Optical Parametric Chirped-Pulse Amplification (OPCPA)-based laser system with a repetition rate of 20 kHz. These pulses propagate nonlinearly through a hollow-core fiber filled with neon gas (at 3.5 bar), generating a supercontinuum that spans from the ultraviolet to the near-infrared spectral range. The broadband spectrum is directed into a light field synthesizer (LFS), as shown in Fig. 1a, where it is split into three spectral channels using dichroic beam splitters: Ultraviolet (UV, 400-500 nm), Visible (VIS, 500-700 nm), and Near-Infrared (NIR, 700-900 nm). Each of these channels is compressed using pairs of chirped

mirrors to approach their Fourier limits. The temporal profiles of the pulses in each channel are shown in Fig. S1. The full width at half maximum (FWHM) pulse durations are 10, 9, and 8.5 fs for the UV, VIS, and NIR pulses, respectively. The pulses are recombined using similar dichroic beam splitters and coherently superimposed at the output of the synthesizer, forming a two-cycle laser pulse. This pulse waveform is finely controlled by adjusting the relative delay between the three LFS pulses with a high-resolution piezoelectric linear stage in the UV and NIR beam paths. Neutral density filters are used to control the relative intensities of the constituent pulses. The total power of the output beam from the LFS is 1W.

The beam is first split using a beamsplitter, with the reflected beam (8% of the total power) representing the classic coherent synthesized pulse. This reflected beam is focused into spectrometer #1 (Ocean Optics HR 4000) with a 5-cm focal length lens. We measure 2800 spectra to assess the average intensity stability (calculated as the mean of each spectrum). Interference fringes between the spectral channels (inset of Fig. 1c and e) are analyzed, and their corresponding Fourier transforms are computed to extract phase jittering between the individual pulses.

The transmitted beam, after passing through the beamsplitter, is directed through a 3-hole mask. The three emerging beams, which are identical in power (162.5 mW), are focused onto a fused silica sample (beam diameter ~ 50 μm , where a four-wave mixing process generates a non-linear light signal which is amplitude-squeezed (0.153 mW). A 1-hole mask filters out this squeezed light, which is then focused into spectrometer #2 (Ocean Optics HR 4000CG) for characterization of its intensity, phase stability, and jitter. The LFS constituent pulses are delayed by hundred femtoseconds to generate better interference fringes at the spectral boundary of each pulse (see in set Fig. 1 c and e)

Next, the relative delay between the LFS channels is also adjusted to synthesize the squeezed light waveform. The waveform is sampled using an all-optical light field sampling technique, reported previously (for further details, see Refs. 24 &25). This method involves focusing the squeezed light onto the SiO₂ sample (200 μm) alongside a probe beam. By measuring the modulation of the probe beam's transmission induced by the squeezed light, we extract the waveform by analyzing the recorded spectrum intensity as a function of the delay between the squeezed light and the probe pulse.

References

- 1 Loudon, R. & Knight, P. L. Squeezed light. *Journal of modern optics* **34**, 709-759, (1987).
- 2 Andersen, U. L., Gehring, T., Marquardt, C. & Leuchs, G. 30 years of squeezed light generation. *Physica Scripta* **91**, 053001, (2016).
- 3 Slusher, R. E., Hollberg, L., Yurke, B., Mertz, J. & Valley, J. Observation of squeezed states generated by four-wave mixing in an optical cavity. *Phys. Rev. Lett.* **55**, 2409, (1985).
- 4 Jia, W. *et al.* Squeezing the quantum noise of a gravitational-wave detector below the standard quantum limit. *Science* **385**, 1318-1321, (2024).
- 5 Aasi, J. *et al.* Advanced ligo. *Classical and quantum gravity* **32**, 074001, (2015).
- 6 Krausz, F. *Electrons in Motion: Attosecond Physics Explores Fastest Dynamics.* (World Scientific Publishing Company Pte. Limited, 2019).

- 7 Corkum, P. & Krausz, F. Attosecond science. *Nat. Phys.* **3**, 381-387, (2007).
- 8 Calegari, F., Sansone, G., Stagira, S., Vozzi, C. & Nisoli, M. Advances in attosecond
science. *J Phys. B At. Mol. Opt. Phys.* **49**, 062001, (2016).
- 9 Christov, I. P., Murnane, M. M. & Kapteyn, H. C. High-harmonic generation of
attosecond pulses in the “single-cycle” regime. *Phys. Rev. Lett.* **78**, 1251, (1997).
- 10 Ghimire, S. *et al.* Observation of high-order harmonic generation in a bulk crystal. *Nat.*
Phys. **7**, 138-141, (2011).
- 11 Luu, T. T. *et al.* Extreme ultraviolet high-harmonic spectroscopy of solids. *Nature* **521**,
498-502, (2015).
- 12 Hentschel, M. *et al.* Attosecond metrology. *Nature* **414**, 509-513, (2001).
- 13 Rasputnyi, A. *et al.* High-harmonic generation by a bright squeezed vacuum. *Nat. Phys.*,
(2024).
- 14 Stammer, P. *et al.* Entanglement and squeezing of the optical field modes in high
harmonic generation. *Phys. Rev. Lett.* **132**, 143603, (2024).
- 15 Tzur, M. E. *et al.* Generation of squeezed high-order harmonics. *Physical Review*
Research **6**, 033079, (2024).
- 16 Rivera-Dean, J. *et al.* Quantum state engineering of light using intensity measurements
and post-selection. *arXiv preprint arXiv:2409.02016*, (2024).
- 17 Rivera-Dean, J. *et al.* Squeezed states of light after high-harmonic generation in excited
atomic systems. *arXiv preprint arXiv:2408.07577*, (2024).
- 18 Ko, D. H. & Corkum, P. Quantum optics meets attosecond science. *Nat. Phys.* **19**, 1556-
1557, (2023).
- 19 Gorlach, A. *et al.* High-harmonic generation driven by quantum light. *Nat. Phys.* **19**,
1689-1696, (2023).
- 20 Gorlach, A., Neufeld, O., Rivera, N., Cohen, O. & Kaminer, I. The quantum-optical
nature of high harmonic generation. *Nature communications* **11**, 4598, (2020).
- 21 Theidel, D. *et al.* Evidence of the Quantum Optical Nature of High-Harmonic
Generation. *PRX Quantum* **5**, 040319, (2024).
- 22 Theidel, D. *et al.* Observation of a Multimode Displaced Squeezed State in High-
Harmonic Generation. *arXiv preprint arXiv:2411.02311*, (2024).
- 23 Even Tzur, M. *et al.* Photon-statistics force in ultrafast electron dynamics. *Nat. Photon.*
17, 501-509, (2023).
- 24 Even Tzur, M. & Cohen, O. Motion of charged particles in bright squeezed vacuum.
Light: Science & Applications **13**, 41, (2024).
- 25 Lemieux, S. *et al.* Photon bunching in high-harmonic emission controlled by quantum
light. *arXiv preprint arXiv:2404.05474*, (2024).
- 26 Heimerl, J. *et al.* Multiphoton electron emission with non-classical light. *Nat. Phys.*, 1-6,
(2024).
- 27 Degen, C. L., Reinhard, F. & Cappellaro, P. Quantum sensing. *Rev. Mod. Phys.* **89**,
035002, (2017).
- 28 Huber, M. *et al.* Stability of person-specific blood-based infrared molecular fingerprints
opens up prospects for health monitoring. *Nature communications* **12**, 1511, (2021).
- 29 Srivastava, A. *et al.* Near-petahertz fieldoscopy of liquid. *Nat. Photon.*, 1-7, (2024).
- 30 Hui, D. *et al.* Attosecond electron motion control in dielectric. *Nat. Photon.* **16**, 33-37,
(2022).
- 31 Alqattan, H., Hui, D., Pervak, V. & Hassan, M. T. Attosecond light field synthesis. *APL*
Photonics **7**, 041301, (2022).

- 32 Hassan, M. T. *et al.* Optical attosecond pulses and tracking the nonlinear response of bound electrons. *Nature* **530**, 66-70, (2016).
- 33 Hassan, M. T. *et al.* Invited Article: Attosecond photonics: Synthesis and control of light transients. *Review of Scientific Instruments* **83**, 111301, (2012).
- 34 Wirth, A. *et al.* Synthesized Light Transients. *Science* **334**, 195-200, (2011).
- 35 Scully, M. O. & Zubairy, M. S. in *Squeezing via nonlinear optical processes* Ch. 4, 460-486 (Cambridge university press, 2001).
- 36 Freyberger, M. & Schleich, W. Phase uncertainties of a squeezed state. *Phys. Rev. A* **49**, 5056, (1994).
- 37 Schleich, W. P. *Quantum optics in phase space*. (John Wiley & Sons, 2015).
- 38 Hui, D. *et al.* Ultrafast optical switching and data encoding on synthesized light fields. *Science Advances* **9**, eadf1015, (2023).
- 39 Hassan, M. T. Lightwave Electronics: Attosecond Optical Switching. *ACS Photonics* **11**, 334-338, (2024).
- 40 Zhang, Y., Bian, Y., Li, Z., Yu, S. & Guo, H. Continuous-variable quantum key distribution system: Past, present, and future. *Applied Physics Reviews* **11**, (2024).
- 41 Qi, B., Lougovski, P., Pooser, R., Grice, W. & Bobrek, M. Generating the local oscillator “locally” in continuous-variable quantum key distribution based on coherent detection. *Physical Review X* **5**, 041009, (2015).

Acknowledgments:

This project is funded by the Gordon and Betty Moore Foundation Grant (GBMF 11476) to M. Hassan. This material is also based upon work partially supported by the Air Force Office of Scientific Research under award number FA9550-22-1-0494.

J.R.D. and M.L. acknowledge support from: European Research Council AdG NOQIA; MCIN/AEI (PGC2018 0910.13039/501100011033, CEX2019-000910 S/10.13039/501100011033, Plan National STAMEENA PID2022-139099NB), project funded by MCIN/AEI/10.13039/501100011033 and by the “European Union Next Generation EU/PRTR” (PRTR-C17.I1), FPI); QUANTERA DYNAMITE PCI2022-132919, Fundació Cellex; Fundació Mir-Puig.Fundació Cellex; Fundació Mir-Puig.

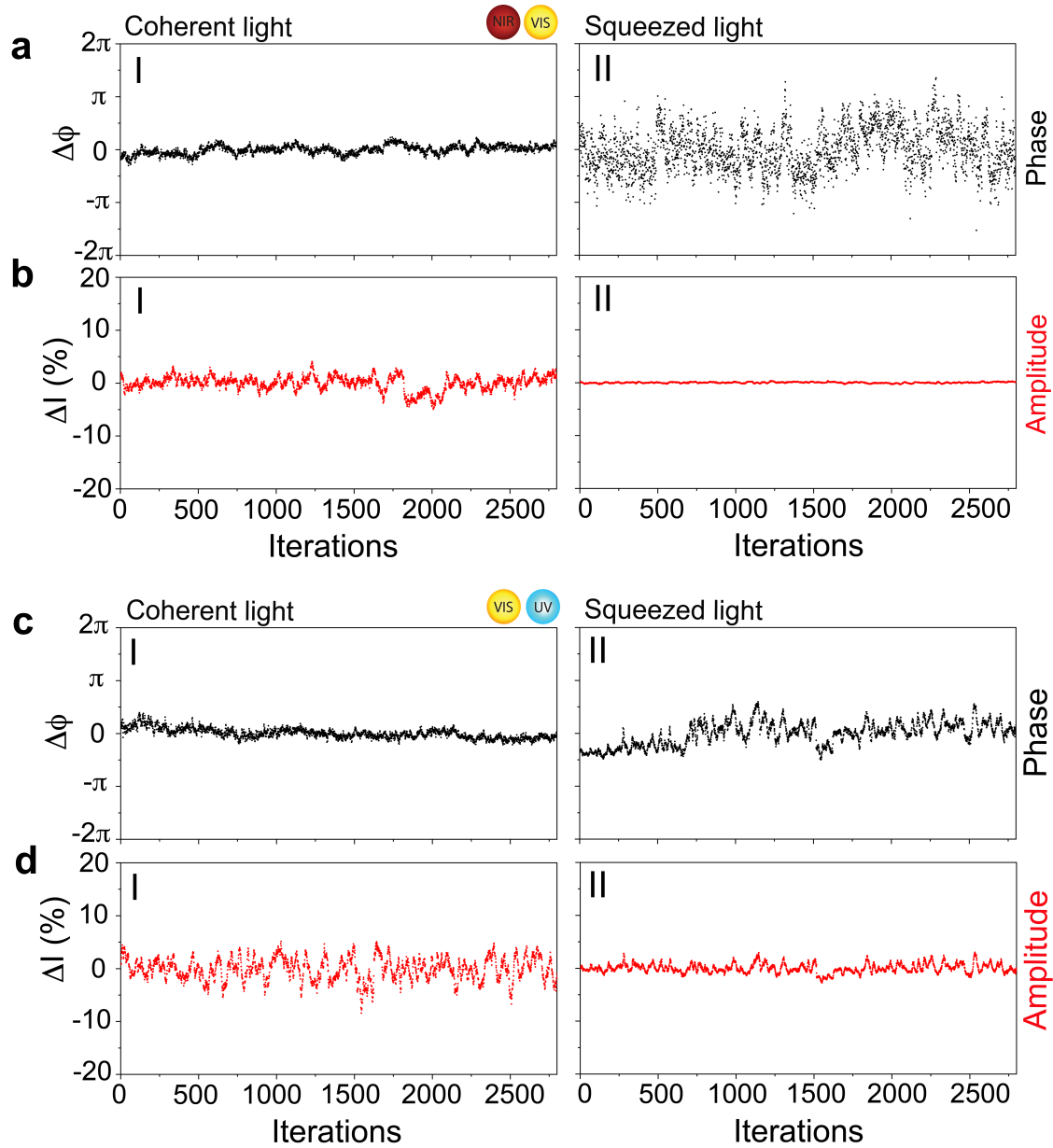


Fig. 2. Squeezed light phase and intensity uncertainty measurements. **a & b**, Measured phase **(a)** and intensity **(b)** uncertainties between the near-IR and visible pulses of the LFS, retrieved by averaging 2800 spectra for classical light **(aI, bI)** and squeezed light **(aII, bII)**. **c&d**, Corresponding phase and intensity uncertainty measurements for the visible and ultraviolet pulses of the LFS, presented in the same order as in panels A and B.

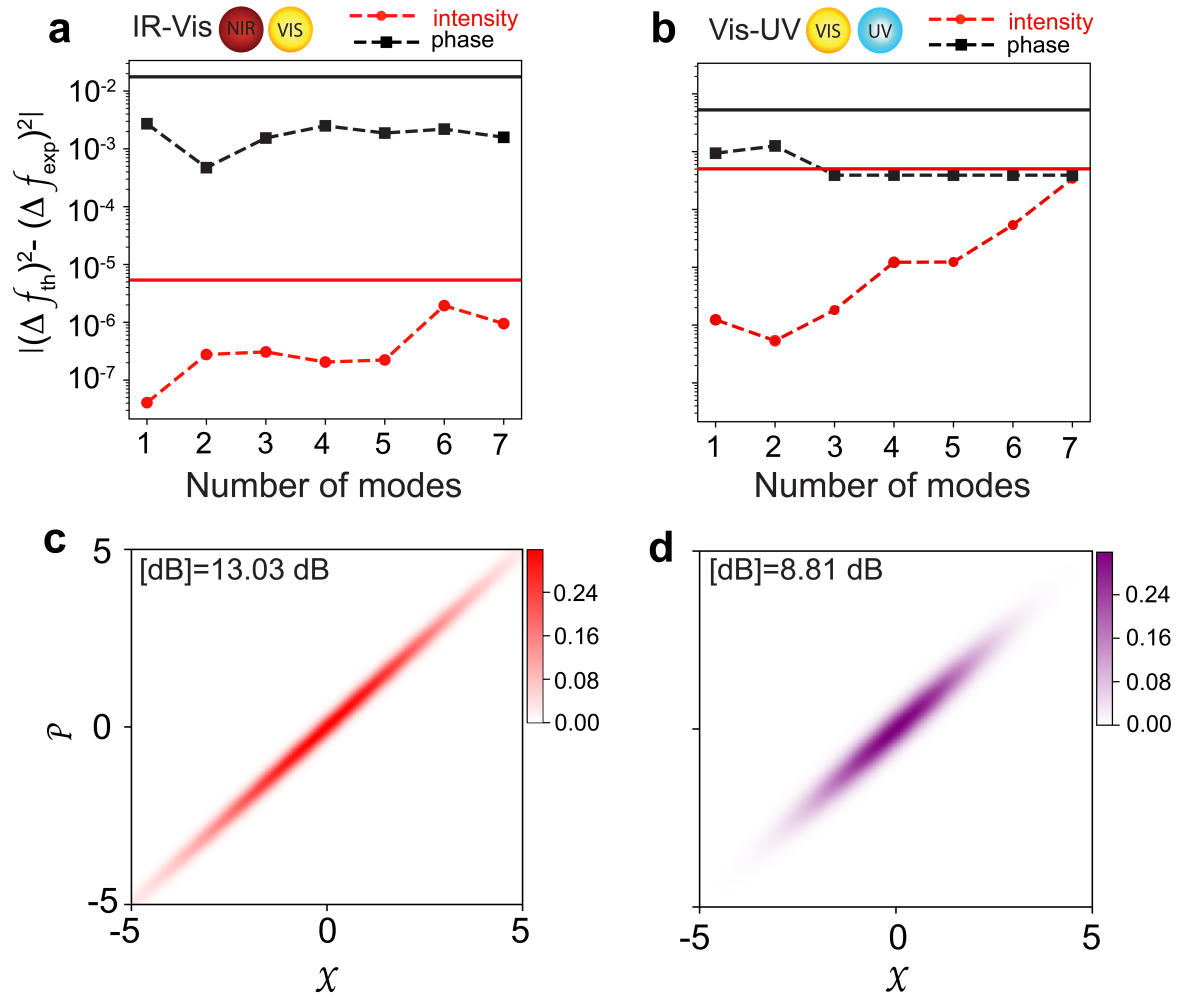


Fig. 3. Wigner functions of the ultrafast squeezed light pulses. a & b, The optimization results for the IR-VIS and UV-VIS datasets as a function of the number of modes. The dashed curves indicate the absolute error between the theoretical and experimental variances for intensity (in red) and phase (in black). For reference, the experimental variances are represented by solid lines in corresponding colors. **c & d,** The Wigner functions of the resulting squeezed states for the IR-VIS and UV-VIS measurements (for $N = 1$), respectively. In these plots, x and p represent the optical quadrature, and for representational purposes, the distributions have been rotated by 45° relative to the p -axis.

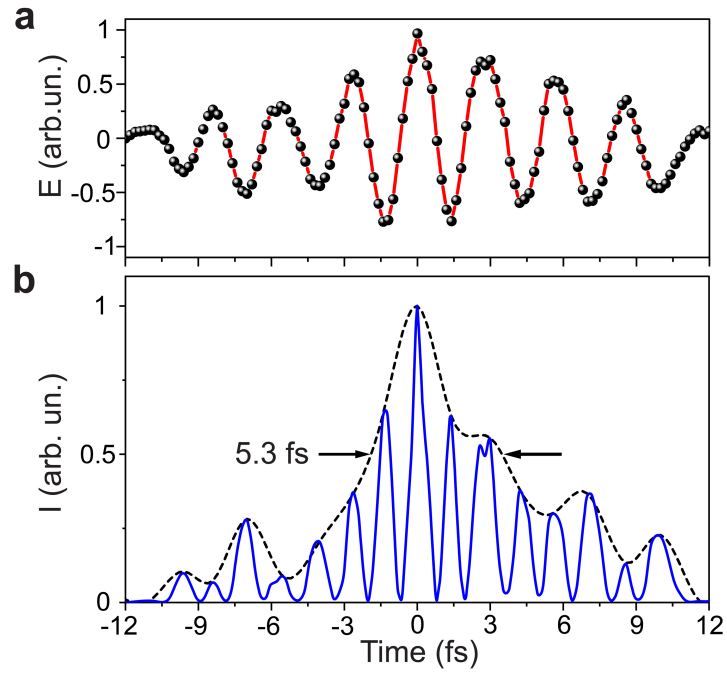


Fig. 4. Ultrafast squeezed light pulse. **a**, Retrieved electric field, and **b**, intensity temporal profile of the ultrafast squeezed light pulse generated by the four-wave mixing nonlinear process of the superimposed three spectral channels of the LFS.

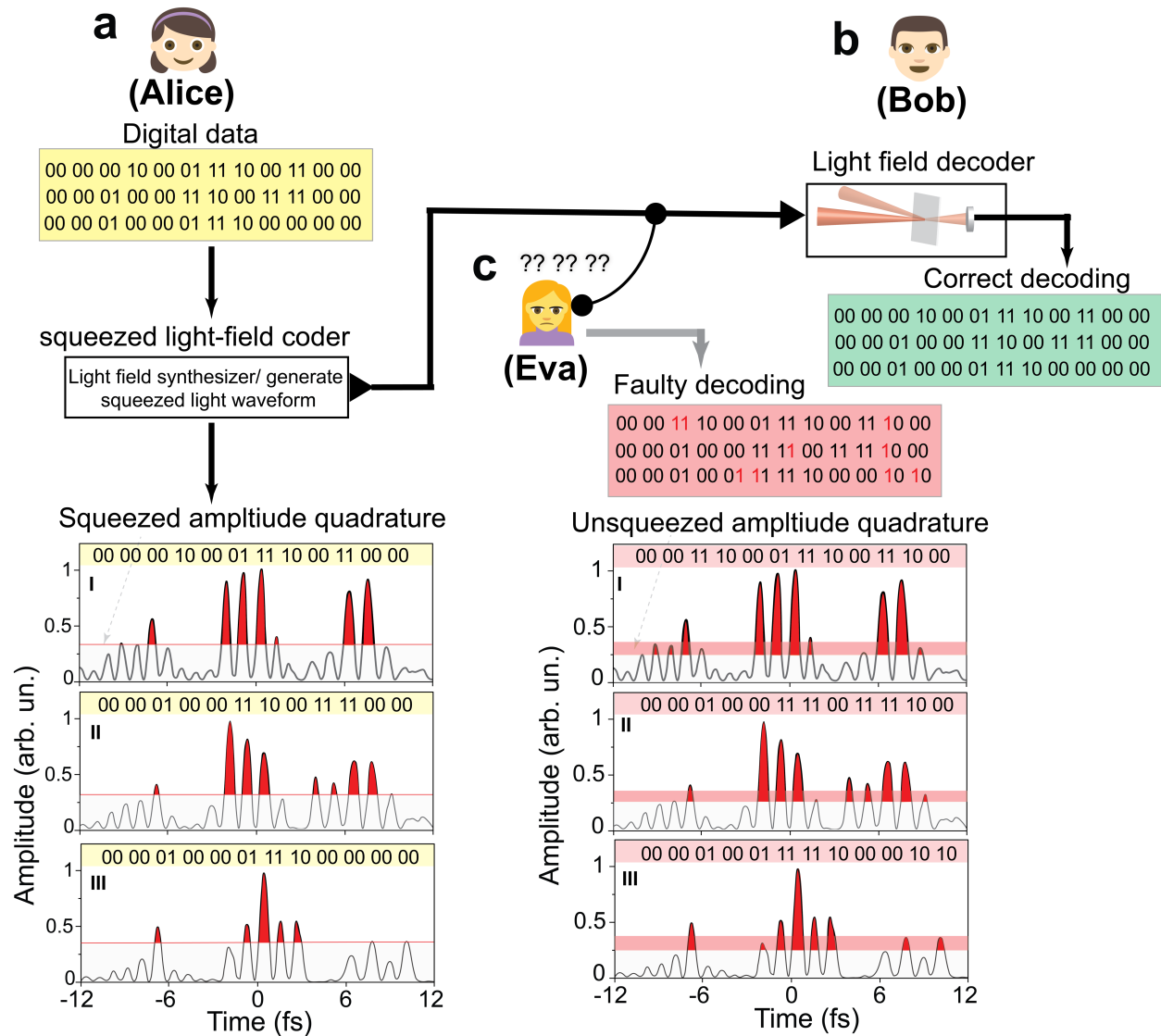


Fig. 5. Ultrafast digital-encoded secure quantum communication. **a**, Alice encodes digital data onto squeezed synthesized light waveforms (**aI-III**) using the LFS. These waveforms have predefined amplitude thresholds, indicated by the red line: signals above the threshold represent (1), and signals below represent (0). The encrypted data are carried by ultrafast squeezed light pulses, which Alice sends to Bob. She also shares the squeezing degree between channels, the predefined threshold, and the encryption key. **b**, Upon receiving the data, Bob first checks the squeezing level to confirm the security of the communication. He then decodes the data by sampling the waveform of the synthesized squeezed light pulses. **c**, Eva attempts to intercept the data using a beamsplitter. Her intervention alters the squeezing level, alerting Alice and Bob to potential tampering. Since Eva does not know the predefined threshold or the data decoding key, her attempt to decode the information results in faulty decoding, as shown in panels **cI-III**.